RSC Advances

PAPER

View Article Online
View Journal | View Issue

Open Access Article. Published on 22 January 2021. Downloaded on 10/31/2025 5:18:51 AM.
This article is licensed under a Creative Commons Attribution-NonCommercial 3.0 Unported Licence.

Check for updates

Cite this: *RSC Adv.*, 2021, **11**, 4610

Regeneration of an electret filter by contact electrification†

Jakyung Eun, Hansol Lee and Sangmin Jeon *

A facile and efficient method for the regeneration of electrostatic potential in electret filters by contact electrification (*i.e.*, triboelectrification) was developed herein. The efficiency of a commercial polypropylene (PP) electret filter (PEF) for face masks was evaluated for filtration of particulate matter (PM) composed of fine solid dust and liquid droplets containing airborne bacteria (bioaerosol). The efficiency of pristine PEF for filtration of fine dust was 72.4%; however, this decreased to 62.7% following the removal of electrostatic charges in PEF by ethanol treatment. In contrast to fine dust, the bioaerosol (BA) removal efficiency of the filter was not affected by ethanol treatment because micro-sized liquid droplets could not penetrate the hydrophobic PEF surface. The electrostatic potential of PEF was restored or even enhanced by rubbing with Teflon, which exhibited a large triboelectric charge density. The PM removal efficiency of the resulting filter was higher than that of pristine PEF. Importantly, no performance degradation was observed even after 10 regenerations, demonstrating that the disposable filter can be reused to reduce the environmental problems associated with accumulation of waste.

Received 18th November 2020
Accepted 15th January 2021

DOI: 10.1039/d0ra09769a

rsc.li/rsc-advances

Introduction

The COVID-19 pandemic is one the most serious threats to global public health in 100 years.[1,2] The pandemic affects not only human health, but also the economy, *e.g.*, due to the suppression of the transportation sector, and thus reduced movement of people and products.[3,4] It is believed that the pandemic can be ended by the development of a commercially available vaccine or medicine. Nonetheless, the discovery of effective prevention or treatment agents may take longer than expected.[5] Consequently, personal hygiene habits, such as washing hands and wearing face masks, are essential to prevent the spread of infectious diseases prior to the development of vaccines or medicines.[6,7]

Medical grade face masks are composed of multiple layers of polypropylene (PP) nonwoven fabrics including electret filters.[8–10] Liquid droplets are blocked by the hydrophobic PP surface,[11] while solid particles are captured by passing through PP fabrics according to the classical filtration theory, *i.e.*, inertial impact, diffusion, and interception.[12–14] Because the average pore size of PP fabrics is larger than tens of micrometers, fine dusts, such as PM2.5 with diameters below 2.5 μm, cannot be effectively captured *via* size-based filtration.[15,16] However, an electret filter produced by a corona discharge on the PP fabric enables efficient capture of particles smaller than the pore size by electrostatic attraction.[17,18]

Despite the proven effectiveness of face masks, their supply did not meet the global demand in the beginning of the COVID-19 pandemic.[19,20] Increased production resulted in sufficient reserves; however, several important issues must be addressed. Firstly, excessive face mask production has become an environmental problem.[21,22] Secondly, a sudden oversupply will cause many companies to go bankrupt, which might lead to another face mask shortage in the future. Notably, the majority of the currently available medical grade face masks are disposable, which leads to unbalanced demand and supply. Consequently, the development of facile and efficient methods for regeneration of disposable face masks is crucial.

Face mask regeneration involves two processes, *i.e.*, cleaning the masks and restoration of their electrostatic charges.[23–25] The former can be easily achieved by washing with ethanol or steam. However, restoration of electrostatic charges is more complex because typical corona discharges require a high voltage power supply, which is not convenient for everyday use at home. We noticed that electrostatic charges can be recovered in the absence of a power supply by contact electrification, *i.e.*, triboelectrification. Because the difference in the normalized triboelectric charge density (TECD) between Teflon (−120 μC m^{-2}) and PP (−25 μC m^{-2}) is quite large,[26] frictional contact between

Department of Chemical Engineering, Pohang University of Science and Technology (POSTECH), 77 Cheongam-Ro, Nam-Gu, Pohang, Gyeongbuk, 37673, Republic of Korea. E-mail: jeons@postech.ac.kr

† Electronic supplementary information (ESI) available: Schematic of the experimental setup to evaluate the PM removal efficiencies for fine dust and bioaerosol; PM removal efficiencies and water contact angles of f-PEF before and after atmospheric Ar plasma treatment; optical microscope images of PEFs washed with hot water (90 °C), steam (100 °C), and aqueous detergent solution (room temperature); surface potentials and PM removal efficiencies of DT-PEF for fine dust; contact angle and PM removal efficiencies of DT-PEF for bioaerosol. See DOI: 10.1039/d0ra09769a

© 2021 The Author(s). Published by the Royal Society of Chemistry

Open Access Article. Published on 22 January 2021. Downloaded on 10/31/2025 5:18:51 AM.
This article is licensed under a Creative Commons Attribution-NonCommercial 3.0 Unported Licence.

them could induce spontaneous electron transfer from Teflon to PP fabrics.[27]

In the present study, we investigated the efficiencies of commercial PP filters for filtration of particulate matter (PM) composed of fine dusts or liquid droplets containing bacteria (*i.e.*, bioaerosol). After cleaning the PP filter by washing with ethanol, the electrostatic potential of the PP filters was regenerated by triboelectrification using a Teflon block. We found that the regenerated filters exhibited similar or higher PM removal efficiencies than pristine filters. This was caused by the higher surface potential of the regenerated filters compared to pristine ones aged on shelves after manufacture. Notably, the regenerated filters retained high PM removal efficiencies during 10 consecutive filtration experiments.

Experimental

Materials

A meltblown PEF was purchased from Gwangil Textile (Daegu, Korea). Arizona fine test dusts (ISO 12103-1 A2 fine grades) were acquired from Powder Technology Incorporated (Minnesota, USA). The concentrations of fine dusts were ~80 μg m^{-3} for $PM_{1.0}$ (PM diameters below 1.0 μm), ~500 μg m^{-3} for $PM_{2.5-1.0}$ (PM diameters between 1.0 and 2.5 μm), and ~1000 μg m^{-3} for $PM_{10-2.5}$ (PM diameters between 2.5 and 10 μm). Ethanol (99.5%) was obtained from Samchun Chemicals (Seoul, Korea). The alconox detergent was purchased from Sigma-Aldrich (Missouri, United States). Deionized (DI) water (18.3 MΩ cm^{-1}) was obtained from a reverse osmosis water system (Human Science, Korea). Teflon sheets (10 cm × 10 cm) and cylindrical blocks (diameter: 4.3 cm, height: 5.6 cm, mass: 57 g) were acquired from Yangzhong Haiteng Fluorine Plastic Product Factory (Shanghai, China) and Vitlab (Grossostheim, Germany), respectively.

Regeneration of PEFs by ethanol washing and triboelectrification

The PEF (4 cm x 4 cm) was immersed in a 70% ethanol solution, gently shaken for 1 min, and subsequently dried in an oven at 60 °C for 20 min. The PEF was then placed on a Teflon sheet and rubbed with a Teflon block for 15 back and forth motion cycles at a speed of 2 cm s^{-1}. The force exerted to the sample measured with an electronic balance during rubbing was 0.56 N. Scheme. 1a illustrates the experimental setup for regeneration of PEF.

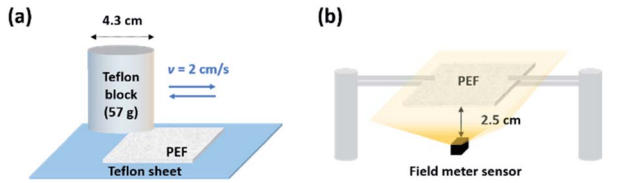

Scheme 1 Schematic of the experimental setup. (a) Regeneration of PEF by triboelectrification. (b) Surface potential measurement.

Characterization of the meltblown PEF

The morphologies of meltblown PEFs were characterized using SEM (JSM-7401F JEOL) and OM (BX53, Olympus). The water contact angle was measured employing SmartDrop (FEMTOFAB, Korea) with 6 μL water droplets. The surface potential of PEF was measured using an electrostatic field meter (ARS-H002ZA, Dongil). Scheme. 1b shows the experimental setup for surface potential measurements. The distance between the PEF sample (4 cm × 4 cm) and the electrostatic field meter was fixed at 2.5 cm to measure the average surface potential of the entire area of the PEF sample.

Evaluation of the efficiencies for the removal of fine dust and bioaerosol (BA)

The efficiency of PEF for the removal of fine dust was assessed in a home-built flow cell[28–30] containing two 250 mL chambers. The PEF was placed between the chambers and a blowing fan was used to drive the Arizona fine dust from one chamber into the other at a rate of 2 L min^{-1} for 10 min (Fig. S1a in the ESI†). The concentrations of fine dusts were measured using a particle counter (PMS7003, PLANTOWER) at the outlet of the second chamber.

The efficiency of PEF for the removal of BA containing 10^6 cfu mL^{-1} *E. coli* was evaluated using a home-built flow cell[31,32] equipped with a nebulizer (Liny AL200, Respironics New Jersey, Inc). The BA produced by the nebulizer was stored in a buffer tank, and allowed to sequentially pass through PEF and commercial PTFE filters with a pore size of 0.45 μm at a flow rate of 0.24 mL min^{-1} for 30 s (Fig. S1b in the ESI†). After conducting the capture experiment in the presence and absence of PEF, each PTFE filter was immersed in a bacterial culture medium (10 mL of LB), sonicated for 2 min, and incubated at 37 °C for 1 h. The culture solution was subsequently diluted and transferred to a solid culture medium, and the bacterial concentration was determined by cell counting.

Results and discussion

Fig. 1a and b show optical microscopy (OM) and scanning electron microscopy (SEM) images of a commercial meltblown PP electret filter (PEF), respectively. The inset of Fig. 1a shows the photo of the f-PEF sample. As demonstrated in Fig. 1c, PP microfibers with diameters ranging from 1 to 10 μm are entangled and stacked to form PEF with a thickness of ~400 μm. The filtration efficiency and pressure drop increased with increasing PEF thickness, *i.e.*, the breathability decreased. High filtration efficiency and low pressure drop are typically achieved by creating electrostatic charges on PEF *via* corona discharge. The electrostatic attraction between the microfibers and PM increases the filtration efficiencies of PEFs, including those exhibiting small thickness and relatively large pores. Despite the presence of electrostatic charges on the PP fibers, the charged surface area is quite small compared to the total surface area (8 charges per 100 nm × 100 nm surface area);[33] therefore, the overall PP surface is hydrophobic. Fig. 1d shows that the water contact angle of fresh PEF (f-PEF) was 146° ± 4.6°.

Open Access Article. Published on 22 January 2021. Downloaded on 10/31/2025 5:18:51 AM.
This article is licensed under a Creative Commons Attribution-NonCommercial 3.0 Unported Licence.

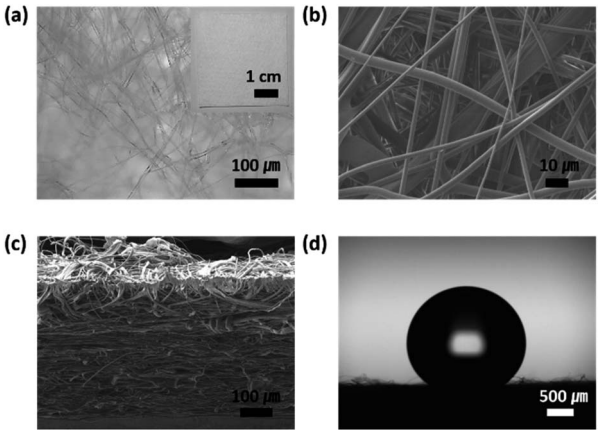

Fig. 1 Magnified images of f-PEP and its wettability toward water. (a) OM image of f-PEF. The inset shows the photo of the f-PEF sample. (b) Top view SEM image of f-PEF. (c) Cross-sectional view SEM image of f-PEF. Various diameters of microfibers were randomly entangled and stacked. (d) OM image of a water droplet on f-PEF. The water contact angle of f-PEF was determined at 146°.

Since the water contact angle of a PP plate with a smooth surface was 96° ± 1.7°, the high water contact angle of f-PEF could be attributed to the roughness of the f-PEF surface, which made it a Cassie-Baxter state.

Efficiencies of PEFs for removal of fine dusts and their regeneration by triboelectrification after ethanol washing

Fig. 2a shows the PM removal efficiencies and surface potentials of various PEFs. Arizona fine dust was used as the PM source and the PM removal efficiency of PEF was assessed by blowing the PM through the filter at a rate of 2 L min^{-1} for 10 min (Fig. S1a in the ESI†). The concentrations of fine dust were determined at ~80 μg m^{-3} for $PM_{1.0}$ (PM diameters below 1.0 μm), ~500 μg m^{-3} for $PM_{2.5-1.0}$ (PM diameters between 1.0 and 2.5 μm), and ~1000 μg m^{-3} for $PM_{10-2.5}$ (PM diameters between 2.5 and 10 μm). The PM removal efficiencies of f-PEF were 72.4%, 87.1%, and 92.9% for $PM_{1.0}$, $PM_{2.5-1.0}$, and $PM_{10-2.5}$, respectively, indicating that the PM removal efficiency of f-PEF increased with increasing PM size.

Fig. 2b shows the OM image of f-PEF following the filtration experiment. While fine dusts were not observed in the image of f-PEF prior to the experiment (Fig. 1a), the OM image of f-PEF after conducting the test showed the presence of a significant amount of fine dust. The fine dusts captured by f-PEF adhered to the microfibers and agglomerated into large solid particles, as shown in the SEM image (Fig. 2c). The captured fine dusts were removed by washing with a 70% ethanol solution. Fig. 2d and e show the OM and SEM images of the PEF after washing with ethanol (E-PEF), respectively. It is noteworthy that the image was nearly identical to that of f-PEF before the experiment. This implied that fine dusts could be completely removed by ethanol washing. In addition, the ethanol treatment did not affect the apparent morphology of PEF, as it was a poor solvent for PP. The PM removal efficiencies of E-PEF were 62.7%, 82.7%, and 91.2% for $PM_{1.0}$, $PM_{2.5-1.0}$, and $PM_{10-2.5}$, respectively, indicating that the efficiencies decreased by 9.7%, 4.4%, and 1.7%, respectively, compared to those of f-PEF. The reduced efficiency of E-PEF was attributed to the decrease in the surface potential following the ethanol treatment. Ethanol washing reduced the surface potential of f-PEF from ~0.9 to ~0.04 kV. Note that the largest decrease in the PM removal efficiency was observed for $PM_{1.0}$, which was consistent with the classical

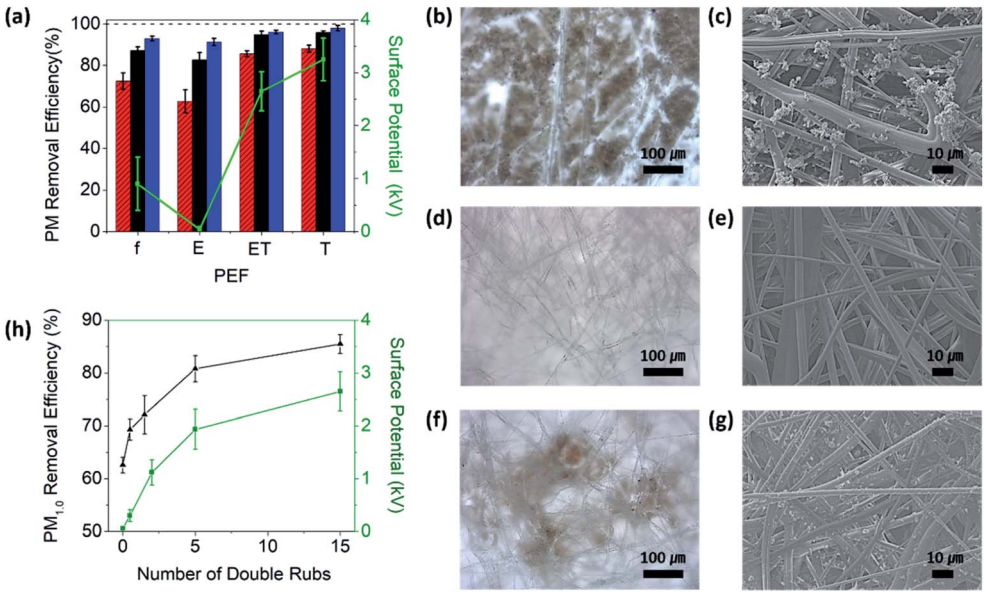

Fig. 2 (a) PM removal efficiencies and surface potentials of PEFs for $PM_{1.0}$ (red), $PM_{2.5-1.0}$ (black), and $PM_{10-2.5}$ (blue). OM and SEM images of (b, c) f-PEF after the filtration experiment, (d, e) E-PEF and (f, g) T-PEF. (h) Variations in the $PM_{1.0}$ removal efficiency and surface potential of ET-PEF as a function of the number of double rubs. The surface potential and $PM_{1.0}$ removal efficiency for number of double rubs 0 were obtained from E-PEF.

 © 2021 The Author(s). Published by the Royal Society of Chemistry

Open Access Article. Published on 22 January 2021. Downloaded on 10/31/2025 5:18:51 AM.
This article is licensed under a Creative Commons Attribution-NonCommercial 3.0 Unported Licence.

filtration theory in that PMs smaller than 1 μm were mostly captured by electrostatic attraction, while those larger than 1 μm by inertial impact and interception.[12]

To regenerate the electrostatic potential of f-PEF, the filter was placed on a Teflon sheet and a Teflon block was moved back and forth over the material to induce triboelectrification (T-PEF). Each back and forth motion cycle represented one double rub. 15 double rubs were applied to regenerate the electrostatic potential of PEF, unless stated otherwise. Since the normalized TECD of Teflon (-120 μC m^{-2}) is significantly larger than that of PP (-25 μC m^{-2}),[26] the frictional contact induced spontaneous electron transfer from Teflon to E-PEF. Note that a surface charge density, which could be obtained by triboelectrification under ambient conditions, is typically 10^{-3} C m^{-2}, corresponding to 8 electrons per 100 nm × 100 nm surface area.[33] The PM removal efficiencies of T-PEF were established at 88.0%, 95.8%, and 97.9% for $PM_{1.0}$, $PM_{2.5-1.0}$, and $PM_{10-2.5}$, respectively (Fig. 2a). The PM removal efficiencies of T-PEF were higher than those of f-PEF and E-PEF because the electrostatic potential of T-PEF (3.2 kV) was greater than those of f-PEF and E-PEF. Nevertheless, the OM and SEM images of T-PEF showed the presence of fine dusts (Fig. 2f and g), which must be removed for safe reuse.

The fine dust accumulated on f-PEF was removed by ethanol washing. Subsequently, the electrostatic potential of E-PEF was regenerated by triboelectrification (ET-PEF). The PM removal efficiencies of ET-PEF were determined at 85.5%, 94.8%, and 96.1% for $PM_{1.0}$, $PM_{2.5-1.0}$, and $PM_{10-2.5}$. Hence, compared to E-PEF, the efficiencies for ET-PEF increased by 22.8%, 12.1%, and 4.9%, correspondingly (Fig. 2a). The PM removal efficiencies of ET-PEF were also higher than those of f-PEF, which was attributed to the larger surface potential of ET-PEF (2.7 kV) than that of f-PEF (0.9 kV). The low surface potential of f-PEF was caused by the gradual degradation of surface charges after fabrication.[34–36] Fig. 2h shows variations in the $PM_{1.0}$ removal efficiency and surface potential of ET-PEF as a function of the number of double rubs. The $PM_{1.0}$ removal efficiency of E-PEF (zero double rub) at the surface potential of 0.04 kV was ~63%. Notably, the electrostatic potential and $PM_{1.0}$ removal efficiency of ET-PEF increased with increasing number of double rubs, reaching 2.7 kV and 85% after 15 double rubs, respectively.

To demonstrate the applicability of ET-PEF for the removal of multiple PM, the PM capture experiment was conducted 10 times. As shown in Fig. 3a, the PM removal efficiencies of ET-PEF remained nearly unchanged, regardless of the number of the capture experiment. This was attributed to the restoration of the surface potential to its original value by triboelectrification, indicating that PEF was not damaged by the ethanol solution and could be effectively reused more than 10 times after ethanol washing. Fig. 3b shows the time dependent change in the surface potential of ET-PEF under ambient conditions (20 °C, 30% RH). The surface potential gradually decreased from 2.9 kV over time, but remained above 2.4 kV for 16 h after regeneration. The high charge stability could be attributed to the intrinsic properties of PP, *i.e.*, high surface resistivity and low surface energy.[36,37]

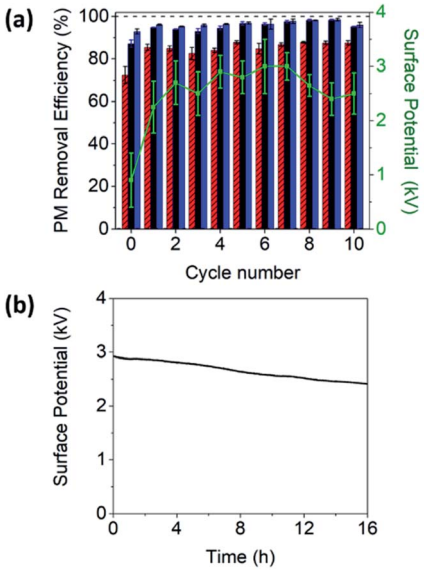

Fig. 3 (a) PM removal efficiencies and surface potentials of ET-PEFs after regeneration. Surface potential (green square) of ET-PEF and its efficiency for the removal of $PM_{1.0}$ (red), $PM_{2.5-1.0}$ (black), and $PM_{10-2.5}$ (blue) in ten consecutive capture experiments. The PM removal efficiency for cycle number 0 was obtained from f-PEF. (b) Time dependent change in the surface potential of ET-PEF under ambient conditions.

Efficiencies of PEFs for removal of BA and their regeneration by triboelectrification after ethanol washing

Bioaerosols are solid particles and liquid droplets released from the soil and water into the atmosphere. They include living and nonliving things, such as bacteria, viruses, fungi, and pollen, and are transported locally or globally by wind or tropical storms.[38] To examine the BA removal efficiency, a spray of an aqueous solution containing 10^6 CFU mL^{-1} of *E. coli* was sequentially passed through PEF and commercial polytetrafluoroethylene (PTFE) filters with a pore size of 0.45 μm (Fig. S1b in the ESI†). After conducting the capture experiment for 30 s in the presence and absence of PEF, each PTFE filter was immersed in lysogeny broth (LB) and the bacterial concentration was determined by cell counting. The BA removal efficiency (η) was calculated according to the following equation:

$$\eta = 1 - \frac{N_{p(w)}}{N_{p(w/o)}} \quad (1)$$

where $N_{p(w)}$ and $N_{p(w/o)}$ indicate the number concentration of bacterial colonies obtained from the PTFE filters with and without PEF, respectively. Fig. 4a shows the BA removal efficiencies of f-PEF, E-PEF, ET-PEF, and T-PEF. All PEFs exhibited BA removal efficiencies of more than 99.9%, regardless of their surface potentials. This is because the aqueous BA did not wet the hydrophobic PEF surface, and was unable to penetrate through the filter. The water contact angles of f-PEF, E-PEF, ET-PEF, and T-PEF were in the range of 145–150°, suggesting that the PEF surfaces were nearly superhydrophobic. In addition, the BA removal efficiencies were ~100%, irrespective of the

Open Access Article. Published on 22 January 2021. Downloaded on 10/31/2025 5:18:51 AM.
This article is licensed under a Creative Commons Attribution-NonCommercial 3.0 Unported Licence.

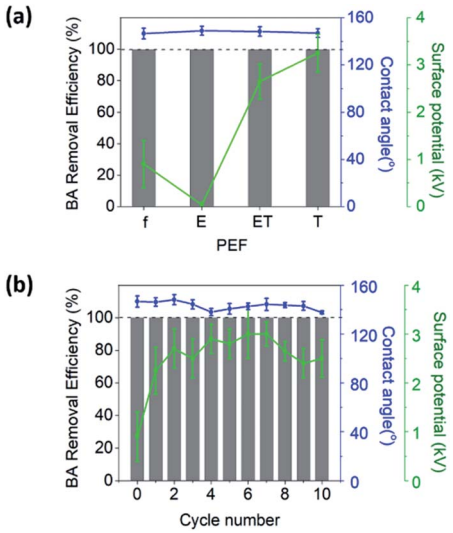

Fig. 4 (a) BA removal efficiencies, water contact angles, and surface potentials of various PEFs. (b) BA removal efficiencies, water contact angles, and surface potentials of ET-PEF during ten consecutive capture experiments.

regeneration cycle number. On the other hand, the water contact angle marginally decreased (Fig. 4b). It is noteworthy that the surface potential recovered to its original value by 15 double rubs, which was analogous to the case of the fine dust capture experiment (Fig. 3a).

A control experiment was conducted to examine the effect of hydrophobicity on the BA removal efficiency. Following irradiation of f-PEF by atmospheric Ar plasma for 30 min, the water contact angle decreased from 146.2° to 125.8° (Fig. S2 in the ESI†) and the BA removal efficiency decreased from 99.9% to 86.4%. This suggested that the water repelling property of PEF played a key role in blocking aqueous liquid BA.

Conclusions

In the present study, we investigated the regeneration of PEF to enable multiple uses of disposable face masks. The regeneration was conducted by triboelectrification following ethanol washing. It was found that ethanol washing removed not only the captured PMs, but also the electrostatic charges of PEF. Nonetheless, the subsequent triboelectrification restored the surface potential of PEF and regenerated its PM removal efficiency. It was found that the surface potential played a key role in trapping fine dusts, while the surface hydrophobicity was significant for blocking liquid BA. Importantly, no performance deterioration, *i.e.*, decrease in the PM removal efficiencies, was observed during 10 consecutive filtration experiments using ET-PEF (Fig. 3a and 4b). PEF can also be cleaned using aqueous detergent solutions instead of ethanol. We confirmed that after rinsing the PEF with water, the surface potential and PM removal efficiency of the filter could be regenerated by triboelectrification (Fig. S3 in the ESI†). The method developed in the current study for the reuse of disposable face masks will make it possible to cope with environmental problems associated with accumulation of waste and unbalanced supply and demand situations.

Conflicts of interest

There are no conflicts to declare.

Acknowledgements

This work was supported by the National Research Foundation of Korea (NRF) grant funded by the Korea government (MSIT; No. 2019R1A5A8080290) and (No. 2019R1A2C1084182).

Notes and references

1 F. Wu, S. Zhao, B. Yu, Y. M. Chen, W. Wang, Z. G. Song, Y. Hu, Z. W. Tao, J. H. Tian, Y. Y. Pei, M. L. Yuan, Y. L. Zhang, F. H. Dai, Y. Liu, Q. M. Wang, J. J. Zheng, L. Xu, E. C. Holmes and Y. Z. Zhang, *Nature*, 2020, **579**, 265–269.
2 N. C. Peeri, N. Shrestha, M. S. Rahman, R. Zaki, Z. Tan, S. Bibi, M. Baghbanzadeh, N. Aghamohammadi, W. Zhang and U. Haque, *Int. J. Epidemiol.*, 2020, **49**, 717–726.
3 M. Nicola, Z. Alsafi, C. Sohrabi, A. Kerwan, A. Al-Jabir, C. Iosifidis, M. Agha and R. Agha, *Int. J. Surg.*, 2020, **78**, 185.
4 B. Pfefferbaum and C. S. North, *N. Engl. J. Med.*, 2020, **383**, 510–512.
5 N. Lurie, M. Saville, R. Hatchett and J. Halton, *N. Engl. J. Med.*, 2020, **382**, 1969–1973.
6 A. Gasmi, S. Noor, T. Tippairote, M. Dadar, A. Menzel and G. Bjørklund, *Clin. Immunol.*, 2020, **215**, 108409.
7 J. Howard, A. Huang, Z. Li, Z. Tufekci, V. Zdimal, H.-M. van der Westhuizen, A. von Delft, A. Price, L. Fridman, L.-H. Tang, V. Tang, G. L. Watson, C. E. Bax, R. Shaikh, F. Questier, D. Hernandez, L. F. Chu, C. M. Ramirez and A. W. Rimoin, *Proc. Natl. Acad. Sci. U. S. A.*, 2021, **118**(4), e2014564118.
8 L. Liao, W. Xiao, M. Zhao, X. Yu, H. Wang, Q. Wang, S. Chu and Y. Cui, *ACS Nano*, 2020, **14**, 6348–6356.
9 J. Carlos Rubio-Romero, M. Del Carmen Pardo-Ferreira, J. Antonio Torrecilla Garcia and S. Calero-Castro, *Saf. Sci.*, 2020, 104830, DOI: 10.1016/j.ssci.2020.104830.
10 P. Forouzandeh, K. O'Dowd and S. C. Pillai, *Saf. Sci.*, 2021, **133**, 104995.
11 S. Sarkar, A. Mukhopadhyay, S. Sen, S. Mondal, A. Banerjee, P. Mandal, R. Ghosh, C. M. Megaridis and R. Ganguly, *Transactions of the Indian National Academy of Engineering*, 2020, **5**, 393–398.
12 G. Liu, M. Xiao, X. Zhang, C. Gal, X. Chen, L. Liu, S. Pan, J. Wu, L. Tang and D. Clements-Croome, *Sustain. Cities Soc.*, 2017, **32**, 375–396.
13 K. Lee and B. Liu, *Aerosol Sci. Technol.*, 1981, **1**, 35–46.
14 K. Lee and B. Liu, *Aerosol Sci. Technol.*, 1982, **1**, 147–161.
15 Y. Pu, J. Zheng, F. Chen, Y. Long, H. Wu, Q. Li, S. Yu, X. Wang and X. Ning, *Polymers*, 2018, **10**, 959.
16 C.-C. Chen and K. Willeke, *Am. J. Infect. Contr.*, 1992, **20**, 177–184.

 © 2021 The Author(s). Published by the Royal Society of Chemistry

Open Access Article. Published on 22 January 2021. Downloaded on 10/31/2025 5:18:51 AM.
This article is licensed under a Creative Commons Attribution-NonCommercial 3.0 Unported Licence.

17 A. Kravtsov, H. Brunig, S. Zhandarov and R. Beyreuther, *Adv. Polym. Technol.*, 2000, **19**, 312–316.
18 M. C. Plopeanu, L. Dascalescu, B. Neagoe, A. Bendaoud and P. V. Notingher, *J. Electrost.*, 2013, **71**, 517–523.
19 H.-l. Wu, J. Huang, C. J. Zhang, Z. He and W.-K. Ming, *EClinicalMedicine*, 2020, **21**, 100329.
20 W. H. Organization, *Newsroom*, 2020, **3**, 2020.
21 M. Shen, S. Ye, G. Zeng, Y. Zhang, L. Xing, W. Tang, X. Wen and S. Liu, *Mar. Pollut. Bull.*, 2020, **150**, 110712.
22 O. O. Fadare and E. D. Okoffo, *Sci. Total Environ.*, 2020, **737**, 140279.
23 R. Lenormand and G. Lenormand, *medRxiv*, 2020, DOI: 10.1101/2020.04.28.20083840.
24 D. J. Viscusi, M. S. Bergman, B. C. Eimer and R. E. Shaffer, *Ann. Occup. Hyg.*, 2009, **53**, 815–827.
25 Q. X. Ma, H. Shan, C. M. Zhang, H. L. Zhang, G. M. Li, R. M. Yang and J. M. Chen, *J. Med. Virol.*, 2020, **92**(9), 1567–1571.
26 H. Zou, Y. Zhang, L. Guo, P. Wang, X. He, G. Dai, H. Zheng, C. Chen, A. C. Wang and C. Xu, *Nat. Commun.*, 2019, **10**, 1427.
27 S. Liu, W. Zheng, B. Yang and X. Tao, *Nano Energy*, 2018, **53**, 383–390.
28 C. Liu, P. C. Hsu, H. W. Lee, M. Ye, G. Zheng, N. Liu, W. Li and Y. Cui, *Nat. Commun.*, 2015, **6**, 6205.
29 S. Jeong, H. Cho, S. Han, P. Won, H. Lee, S. Hong, J. Yeo, J. Kwon and S. H. Ko, *Nano Lett.*, 2017, **17**(7), 4339–4346.
30 H. Liu, J. Huang, J. Mao, Z. Chen, G. Chen and Y. Lai, *iScience*, 2019, **19**, 214–223.
31 W. Jing, W. Zhao, S. Liu, L. Li, C. Tsai, X. Fan, W. Wu, J. Li, X. Yang and G. Sui, *Anal. Chem.*, 2013, **85**, 5255–5262.
32 M. G. Stanford, J. T. Li, Y. Chen, E. A. McHugh, A. Liopo, H. Xiao and J. M. Tour, *ACS Nano*, 2019, **13**, 11912–11920.
33 Z. L. Wang and A. C. Wang, *Mater. Today*, 2019, **30**, 34–51.
34 B. Tabti, M. R. Mekideche, M.-C. Plopeanu, L. M. Dumitran, L. Herous and L. Dascalescu, *IEEE Trans. Ind. Appl.*, 2010, **46**, 634–640.
35 H. Gao, W. He, Y.-B. Zhao, D. M. Opris, G. Xu and J. Wang, *J. Membr. Sci.*, 2020, **600**, 117879.
36 J. Lee and J. Kim, *Polymers*, 2020, **12**, 721.
37 E. Nemeth, V. Albrecht, G. Schubert and F. Simon, *J. Electrost.*, 2003, **58**, 3–16.
38 J. Fröhlich-Nowoisky, C. J. Kampf, B. Weber, J. A. Huffman, C. Pöhlker, M. O. Andreae, N. Lang-Yona, S. M. Burrows, S. S. Gunthe and W. Elbert, *Atmos. Res.*, 2016, **182**, 346–376.